THE JOURNAL OF BIOLOGICAL CHEMISTRY VOL. 288, NO. 24, pp. 17451–17459, June 14, 2013

X-ray Structure Analysis and Characterization of AFUEI, an Elastase Inhibitor from *Aspergillus fumigatus*[*] [S]

Received for publication, November 13, 2012, and in revised form, April 21, 2013 Published, JBC Papers in Press, May 2, 2013, DOI 10.1074/jbc.M112.433987

Mayuko Sakuma[‡], Katsumi Imada[§], Yoshiyuki Okumura[¶], Kei-ichi Uchiya[¶], Nobuo Yamashita[‖], Kenji Ogawa[**], Atsushi Hijikata[‡‡], Tsuyoshi Shirai[‡‡], Michio Homma[‡1], and Toshiaki Nikai[¶]

From the [‡]Division of Biological Science, Graduate School of Science, Nagoya University, Furo-cho, Chikusa-Ku, Nagoya 464-8602, Japan, [§]Department of Macromolecular Science, Graduate School of Science, Osaka University, Machikaneyama 1-1, Toyonaka 560-0043, Japan, [¶]Department of Microbiology, Faculty of Pharmacy, Meijo University, 150 Yagotoyama, Tempaku-ku, Nagoya 468-8503, Japan, [‖]Hakutsuru Sake Brewing Co. Ltd, Sumiyoshiminami-machi, Higashinada-Ku, Kobe 658-0041, Japan, [**]Department of Pulmonary Medicine, Higashi Nagoya National Hospital, 5-101 Umemorizaka, Meito-Ku, Nagoya 465-8620, Japan, and the [‡‡]Faculty of Bioscience, Nagahama Institute of Bio-Science and Technology, 1266 Tamura, Nagahama, 526-0829 Japan

Background: Elastase is an important factor in aspergillosis, and AFUEI is an elastase inhibitor derived from *Aspergillus fumigatus.*
Results: The structure of AFUEI, the first structure of the I78 inhibitor family, was determined.
Conclusion: The structure of AFUEI is extremely similar to serine protease inhibitors of the potato inhibitor I family.
Significance: Our findings provide a basic contribution to both the prevention and treatment for aspergillosis.

Elastase from *Aspergillus sp.* is an important factor for aspergillosis. AFUEI is an inhibitor of the elastase derived from *Aspergillus fumigatus*. AFUEI is a member of the I78 inhibitor family and has a high inhibitory activity against elastases of *Aspergillus fumigatus* and *Aspergillus flavus*, human neutrophil elastase and bovine chymotrypsin, but does not inhibit bovine trypsin. Here we report the crystal structure of AFUEI in two crystal forms. AFUEI is a wedge-shaped protein composed of an extended loop and a scaffold protein core. The structure of AFUEI shows remarkable similarity to serine protease inhibitors of the potato inhibitor I family, although they are classified into different inhibitor families. A structural comparison with the potato I family inhibitors suggests that the extended loop of AFUEI corresponds to the binding loop of the potato inhibitor I family, and AFUEI inhibits its cognate proteases through the same mechanism as the potato I family inhibitors.

Protein inhibitors of proteinases produced by animals, plants, and microorganisms are highly specific and have physiological functions to prevent unwanted proteolysis (1). Currently the proteinase inhibitors are grouped into 71 families based on their amino acid sequences and 34 clans based on their structure (2). Some of the inhibitors are important for treating diseases, but details about the physiological functions for many of the inhibitors are not fully understood.

Aspergillosis is an opportunistic infection and is a common mycosis in immunocompromised hosts undergoing chemotherapy (3, 4). Elastases produced by *Aspergillus fumigatus* and *Aspergillus flavus* are thought to be major pathogenic factors in aspergillosis (5, 6). *Aspergillus oryzae* and *Aspergillus sojae* also produce elastases, which are important for the production of fermented foods (7–9). Elastase is a serine proteinase that cleaves on the carboxyl side of small hydrophobic residues and belongs to the same proteinase family as trypsin and chymotrypsin.

An inhibitor of elastases was isolated during the purification of elastase from *A. flavus* and was named AFLEI (*A. flavus* elastase *i*nhibitor) (10). Recently, a similar elastase inhibitor was identified from *A. fumigatus* (AFUEI, *A. fumigatus* elastase *i*nhibitor), and its amino acid sequence was identical to that of AFLEI (11, 12). AFUEI is synthesized with an N-terminal 19-amino acid peptide that was predicted as a signal peptide, and mature AFUEI is composed of 68 amino acid residues. AFUEI strongly inhibits the elastolytic activity of elastases from *A. flavus*, *A. fumigatus*, and human neutrophils, as compared with other elastase inhibitors that have been used in previous studies or in clinical trials (10, 13). AFUEI does not inhibit either thrombin or Ac1 proteinase from snake venom (14). AFUEI is classified into the I78 inhibitor family in the MEROPS database (15), but the structure and the physiological roles of this inhibitor family are not known.

Here we report the high resolution structure of AFUEI, the first structure of the I78 inhibitor family. The structure of AFUEI is similar to those of the potato inhibitor I family members. They are classified into the I13 inhibitor family and the IG clan in the MEROPS database. We discuss the inhibitory mechanism of the I78 inhibitor family and the relationship between the I78 and the potato inhibitor I family.

* This work was supported in part by grants-in-aid for scientific research from the Ministry of Education, Science, and Culture of Japan and from the Japan Science and Technology Corporation (to M. H.) and for Specially Promoted Research of Meijo University Research Institute and from the Yakult Co. Ltd. (to T. N.). This work was also supported by the Platform for Drug Discovery, Informatics, and Structural Life Science from the Ministry of Education, Culture, Sports, Science, and Technology, Japan (to A. H. and T. S.).

[S] This article contains supplemental Figs. S1–S3.

The atomic coordinates and structure factors (codes 3W0D and 3W0E) have been deposited in the Protein Data Bank (http://wwpdb.org/).

[1] To whom correspondence should be addressed. Tel.: 81-52-789-2991; Fax: 81-52-789-3054; E-mail: g44416a@cc.nagoya-u.ac.jp.

TABLE 1
Summary of the diffraction data statistics
Values in parentheses indicate statistics for the highest resolution shell.

Data collection parameters	Form I native	Osmium derivative	Form II native
Space group	$P6_5$	$P6_5$	*H32*
Unit-cell parameters (Å, °)	$a = b = 40.7$ $c = 135.5$ $\gamma = 120$	$a = b = 40.5$ $c = 134.8$ $\gamma = 120$	$a = b = 77.5$ $c = 115.2$ $\gamma = 120$
Wavelength	1.000	1.000	1.000
Resolution (Å)	35.2-2.3 (2.42-2.3)	35.1-2.3 (2.42-2.3)	32.2-1.8 (1.9-1.8)
Observations	22,661 (3300)	72,195 (10604)	114,456 (16,123)
Unique reflections	5,612 (825)	5,502 (806)	12,564 (1,813)
Completeness (%)	99.2 (99.2)	98.6 (99.2)	99.8 (100)
Redundancy	4.0 (4.0)	13.1 (13.2)	9.1 (8.9)
$I/\sigma(I)$	4.7 (2.5)	3.9 (2.5)	5.2 (1.9)
R_{merge} (%)	10.7 (30.0)	13.8 (28.6)	8.0 (40.1)
R_{anom} (%)		6.0 (9.6)	

EXPERIMENTAL PROCEDURES

Purification and Crystallization of AFUEI—Details of the expression and purification of AFUEI were previously described (16). The protein solution for crystallization was prepared by dissolving vacuum-dried AFUEI in distilled water (19 mg/ml). Crystal screening was performed by the sitting-drop vapor-diffusion technique with commercially available screening kits Wizard I and II (Emerald BioSystems) and Crystal Screen I and II (Hampton Research). Each drop was prepared by mixing 0.2 μl of protein solution with 0.2 μl of reservoir solution and equilibrated to a 100-μl reservoir solution. After optimizing the crystallization conditions, we obtained two crystal forms, Form I and Form II, that are suitable for x-ray analysis.

Form I crystals were grown from drops containing 1.4–1.5 M NaCl and 10% (v/v) ethanol at 293 K. Needle-like hexagonal cylinder crystals appeared in 2–3 days and grew to typical dimensions of 0.01 × 0.01 × 0.5 mm within a week. The space group of the crystals was hexagonal $P6_5$ with unit cell dimensions $a = b = 40.7$ Å and $c = 135.5$ Å. Osmium derivative crystals were prepared by soaking the crystals in a reservoir solution containing K_2OsCl_6 at 50% saturation for 4 h.

Form II crystals were grown from drops containing 0.6–1.0 M sodium sulfate, 0.1 M acetate buffer at pH 4.0. Tetragonal crystals appeared in 1 day and grew to maximum dimensions of 0.04 × 0.04 × 0.04 mm in a week. The space group of the crystals was *H32* with unit cell dimensions $a = b = 77.5$ Å and $c = 115.2$ Å.

Data Collection and Structure Determination—X-ray diffraction data were collected at the synchrotron beamlines BL32XU and BL41XU in SPring-8 (Harima, Japan). Crystals were soaked into a cryo-protectant solution containing 10% (v/v) glycerol and 90% (v/v) of the reservoir solution for a few seconds and were then immediately transferred into liquid nitrogen for freezing. The x-ray diffraction data were collected under nitrogen gas flow at 90 K. The statistics of the diffraction data are summarized in Table 1.

The diffraction data were processed and scaled with MOSFLM (17) and SCALA (18), respectively. The initial SAD phase was calculated with the program PHENIX (19) using the osmium derivative data of the Form-I crystal. The atomic model of Form-I was constructed with Coot (20) and refined to 2.3 Å with CNS (21). The refinement R factor and the free R factor were converged to 20.5 and 25.2%, respectively. The Ramachandran plot indicated that 93.3 and 6.7% residues were located in the most favorable and allowed region, respectively. The structure of the Form-II crystal was solved by molecular replacement with the program PHENIX using the coordinate of subunit A in Form-I as a search model. The model was modified with Coot and refined to 1.8 Å resolution with the program PHENIX. The R factor and the free R factor were converged to 21.1 and 25.6%, respectively. The Ramachandran plot showed that 92.5 and 7.5% residues were located in the most favorable and allowed region, respectively. The structural refinement statistics are summarized in Table 2.

Size Exclusion Chromatography—Analytical size exclusion chromatography was performed with a Superdex 75 5/150 GL column (GE Healthcare) connected to a ÄKTA system (GE Healthcare). The column was equilibrated with buffer containing 50 mM Tris-HCl (pH 8.0), and elution was performed at a flow rate of 0.5 ml/min.

Inhibitory Assay for Proteinase Activity—Proteolytic activity was assayed using 2% (w/v) casein as the substrate. Casein was dissolved in 50 ml of 0.4 M Tris-HCl buffer (pH 8.5) by heating for 15 min in a boiling water bath. 0.1 ml of the AFUEI solution was mixed with 0.4 ml of enzyme solution (chymotrypsin, trypsin, and porcine pancreas elastase) and incubated for 15 min at 37 °C. Then 0.5 ml of the 2% casein solution was added and further incubated for 15 min at 37 °C. The reaction was stopped by the addition of 1 ml of 0.44 M trichloroacetic acid. After 30 min, the mixture was filtered. A 0.5-ml aliquot of the filtrated solution was mixed with 2.5 ml of 0.4 M sodium carbonate and 0.5 ml of 2-fold diluted Folin reagent. The absorbance of the mixture was then measured at 660 nm.

Molecular Modeling of the Complex Structure of AFUEI and Human Neutrophil Elastase (HNE)[2]—The template structure for the complex model was searched using Structure-Interaction Relational Database (SIRD) system. The crystal structure of the rBTI (recombinant buckwheat trypsin inhibitor)-trypsin complex (PDB ID 3RDZ) (22) was found to be the best template, as the inhibitor BTI and the enzyme trypsin showed the highest similarity to AFUEI (14% identity in amino acid sequence and

[2] The abbreviations used are: HNE, human neutrophil elastases; *dN*/*dS*, nonsynonymous/synonymous substitution rate; CI-2, chymotrypsin inhibitor-2; rBTI, recombinant buckwheat trypsin inhibitor.

TABLE 2
Refinement statistics
Values in parentheses indicate statistics for the highest resolution shell.

Measurement	Form I	Form II
Resolution range (Å)	31.28-2.3 (2.44-2.3)	32.22-1.8 (1.87-1.8)
No. of reflections working	5,612 (843)	11,308 (1199)
No. of reflections test	544 (94)	1,241 (164)
R_w (%)	20.5 (25.1)	21.1 (27.5)
R_{free} (%)	25.2 (29.6)	25.6 (30.8)
Root mean square deviation bond length (Å)	0.009	0.009
Root mean square deviation bond angle (°)	1.6	1.1
B factors		
Protein atoms	26.5	25.5
Solvent atoms	35.9	34.6
Ramachandran plot (%)		
Most favored allowed	93.3	92.5
Additionally allowed	6.7	7.5
Generously allowed	0.0	0.0
Disallowed	0.0	0.0
No. of protein atoms	1052	1052
No. of solvent atoms	104	174

4.8 Å root mean square deviation for Cα atom superposition) and HNE (23) (32% identity in amino acid sequence and 2.3 Å root mean square deviation for Cα atom superposition), respectively.

The atomic coordinates of AFUEI and HNE (PDB ID 2Z7F) were superimposed on those of the inhibitor and enzyme in the template structure by using MOE (Chemical Computing Group, Inc.). The amino acid sequences of HNE (Ile-16–Gln-243) and trypsin (Ile-19–Asn-241) were aligned with gaps to determine the equivalent residue pairs, and the Cα atoms of 207 equivalent residue pairs were superimposed. The Cα atoms of Pro-33–Gln-55 residues of AFUEI were superimposed to the Cα atoms of Arg-33–Phe-55 of BTI. A water molecule bound to the backbone atoms of Thr-44 (P_2) and Asp-46 (P_1') of AFUEI was included in the complex structure.

The model structure was then optimized by energy minimization calculation using MOE. We assume that AFUEI binds to HNE through the same inhibitory mechanism as potato I family inhibitors, which is called the clogged gutter mechanism (24). According to the mechanism, the hydroxy group of Ser-195 in HNE is thought to act as a nucleophile to Met-45 (P_1) C to form acyl-enzyme complex with AFUEI. The side-chain atoms of Met-45 (P_1) would interact with residues in the hydrophobic active site pocket of HNE. The residues in the extended loop would make main-chain hydrogen bonds with HNE as observed in the complex structures of potato I family inhibitors and proteases (22, 26). We thus performed an energy minimization calculation with the following distance restraints: Met-45 (P_1) Cϵ–Ala-187 Cβ (4.0 Å), Ile-43 (P_3) O–Val-190N (2.8 Å), Ile-43 (P_3) N–Val-190 O (2.8 Å), Met-45 (P_1) N–Ser-188 O (2.8 Å), Met-45 (P_1) C– Ser-195 Oγ (2.6 Å).

Phylogenic Analysis of Potato I Family Inhibitors and AFUEI—The amino acid sequences of potato I family inhibitors were retrieved from the UniProt database by the BLAST program (25). For the query sequences, we used the six amino acid sequences of the inhibitors whose three-dimensional structures are known: Eglin-C (PDB ID 1ACB) (26), bitter gourd trypsin inhibitor BGIT (PDB ID 1VBW), chymotrypsin inhibitor-2 (CI-2; PDB ID 2CI2) (27), buckwheat trypsin inhibitor BTI (PDB ID 3RDZ) (22), *Linum usitatissimum* trypsin inhibitor LUTI (PDB ID 1DWM) (28), and *Cucurbita maxima* trypsin inhibitor V CMTI-V (PDB ID 1MIT) (29). ALAdeGAP (30) was used for multiple sequence alignment of the amino acid sequences of the potato I family inhibitors and AFUEI. A phylogenic tree was drawn with Neighbor-joining method using Phylip 3.69 package. The reliability for each branch of the tree was evaluated by the bootstrap method implemented in ClustalW (31).

The selected amino acid sequences were back-translated into DNA sequence, and the alignment was used for non-synonymous/synonymous substitution rate (*dN*/*dS*) analysis by using PAML (32). A F1X4 matrix was used for the codon substitution model with the universal codon table. The free *dN*/*dS* ratio with M8 (β and ω) model was adapted.

RESULTS AND DISCUSSION

Overall Structure of AFUEI—AFUEI was crystallized in two different forms; Form I with the space group $P6_5$ and Form II with the space group *H*32. We determined the crystal structures of Form I and Form II at 2.3 and 1.8 Å resolution, respectively. The AFUEI molecules in the two crystal forms adopt basically the same structure. Both crystal forms contain two AFUEI molecules in an asymmetric unit. The two molecules are related by pseudo 2-fold rotational symmetry and adopt almost identical conformations. The structure models contain all amino acid residues of the mature AFUEI (Asp-1– Ala-68). AFUEI is a wedge-shaped protein composed of two α-helices (α1 and α2) and four β-strands (β1-β4) (Fig. 1*A*). The core of the molecule contains an α/β sandwich motif consisting of the two α-helices and a mixed β-sheet of three strands, β1, β3, and β4. α1 is tightly connected with β4 through a disulfide bond between Cys-5 and Cys-67. A segment from Gly-40 to Ala-49 protrudes from the core and forms the tip of the wedge. β2, which is present in the middle of this segment, forms an intermolecular β-sheet with β2 of the adjacent molecule related by local pseudo 2-fold symmetry (Fig. 1*B*). Thus the two molecules in the asymmetric unit seem to be a dimer. Size exclusion chromatography analysis, however, indicated that the apparent molecular weight of AFUEI in solution is ~7,000 (Fig. 2), suggesting that AFUEI is a monomer in solution and the dimer is a crystal packing artifact.

AFUEI Structure Resembles the Inhibitors of the Potato Inhibitor I Family—AFUEI shows remarkable structural similarity to the potato inhibitor I family proteins, which is one of the most well studied protease inhibitor families (Fig. 3). Most of the known structures in this family are of plant origin, such as barley wheat CI-2 (33), BTI (22), *L. usitatissimum* trypsin inhibitor (LUTI) (27) and *C. maxima* trypsin inhibitor V (CMTI-V) (29). The exceptions are Eglin-C, which is derived from the leech *Hirudo medicinalis* (26, 34), and LTCI from the earthworm *Lumbricus terrestris* (35). The potato I family inhibitors share a common α/β sandwich core with an extended loop containing a β-strand in its middle. These structural features are perfectly conserved in AFUEI (Fig. 3). Although AFUEI shows low sequence identity with potato I family inhibitors, only the extended loop region is highly conserved (Fig. 4). The loop region of AFUEI shows 55.6% identity to the corresponding residues of

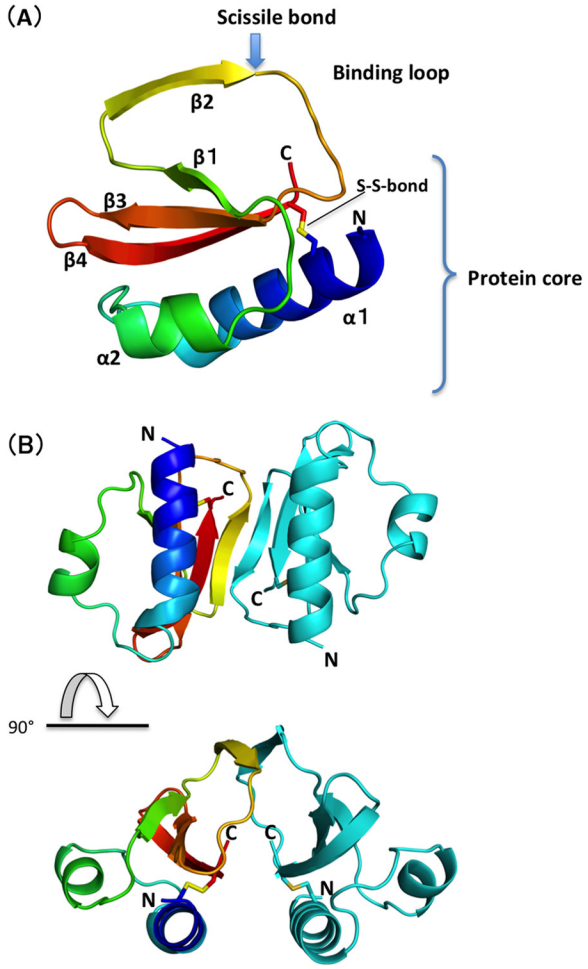

FIGURE 1. **Overall structure of AFUEI.** *A*, shown is a ribbon representation of the crystal structure of AFUEI (Form II) in rainbow colors from the N terminus (*blue*) to the C terminus (*red*). *B*, the AFUEI dimer in the crystallographic asymmetric unit (Form II) is shown. Two AFUEI molecules are shown by the multicolored and *cyan* structure. The disulfide bond is indicated by a *yellow stick*. The *lower panel* is viewed from the top of the upper panel.

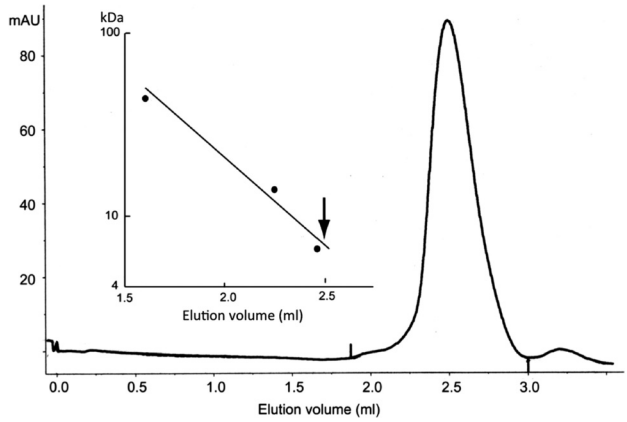

FIGURE 2. **Analytical gel-filtration chromatography of AFUEI.** Elution profile of purified AFUEI. The *inset* indicates the calibration curve for the column (Superdex 75 5/150 GL) using a mixture of standard proteins of ovalbumin (43 kDa), ribonuclease A (13.7 kDa), and aprotinin (6.5k Da). The elution peak position of AFUEI is indicated by an *arrow*.

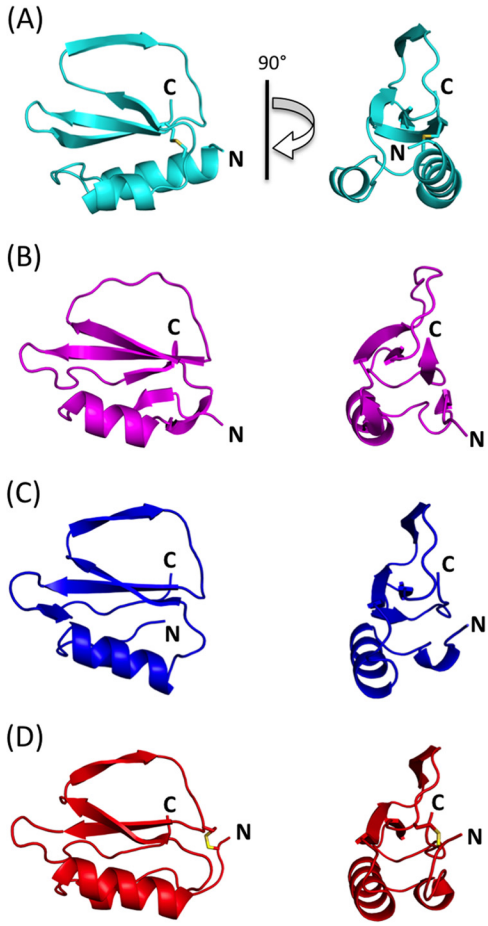

FIGURE 3. **Comparison of the structures of AFUEI and potato I family inhibitors.** Ribbon diagrams of AFUEI (Form II) (*A*), CI-2 (PDB ID 2CI2) (*B*), eglin-c (elastase inhibitor of the leech *H. medicinalis,* PDB ID 1ACB) (*C*), and rBTI (PDB ID 3RDY) (*D*) are shown. The *right panels* are viewed from the right of the left panels. The disulfide bonds are indicated by a *yellow stick*.

CI-2 but 11.9% for the remaining ones. The potato I family inhibitors hamper their cognate protease by tightly fitting the extended loop into the protease active site. Thus the loop is called the "binding loop." The structural and sequence similarities suggest that AFUEI also uses the loop for protease inhibition.

Although the overall structure of AFUEI is similar to that of the potato I family inhibitors, two major structural differences were found between them. One is the size of α1 and α2. α1 is longer than α2 in AFUEI but is shorter in the potato I family inhibitors. The N-terminal region of α1 in the potato I family inhibitors is disordered. The other difference is the position of the disulfide bridge. The disulfide bond of AFUEI connects α1 and β4, whereas in the potato inhibitor I family it bridges the N-terminal loop and the end of the binding loop. Some of the potato I family inhibitors do not have a disulfide bond. However, the disulfide bond contributes significantly to the inhibitory activity of AFUEI. In fact, chemically synthesized AFUEI, which does not form a disulfide bond, has less inhibitory activity to elastase (data not shown). These structural properties indicate that the structure of AFUEI is more compact and rigid than the known potato I family inhibitors.

The Binding-loop Structure—The substrate residues accommodated in proteases are numbered from the scissile bond; P_1, $P_2 \ldots P_n$ toward the N terminus of substrates, P_1', $P_2' \ldots P_n'$ toward the C terminus (1). The same naming rule is applied for inhibitors. The residues at P_6– P_3' of the potato I family inhib-

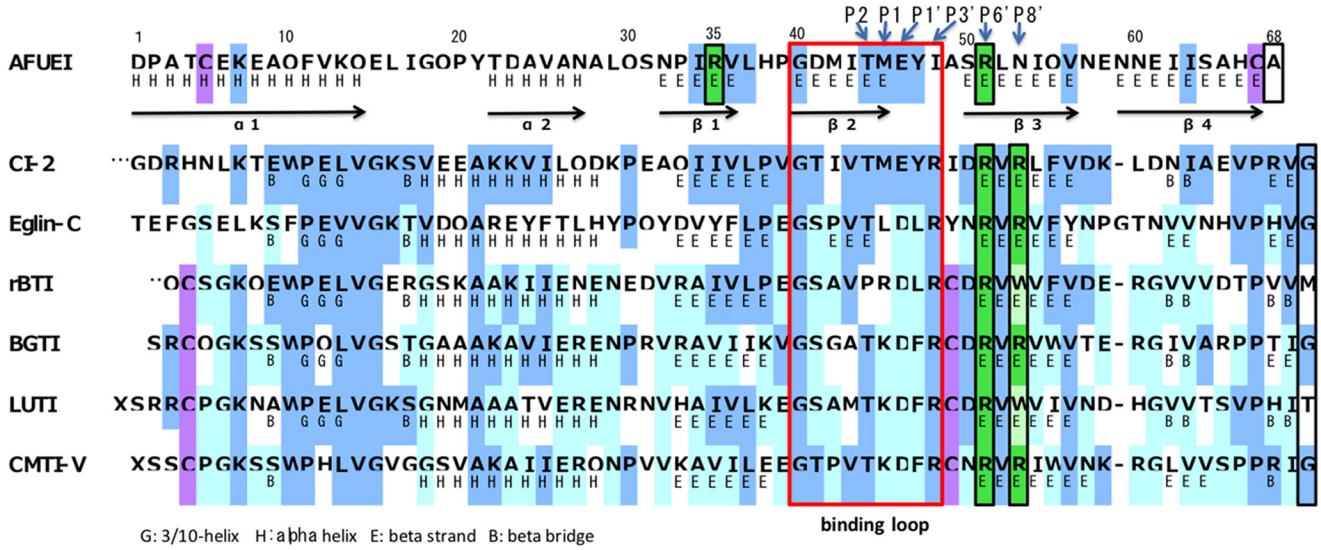

FIGURE 4. **Structure based sequence alignment of AFUEI and potato I family inhibitors.** The amino acid sequences of AFUEI, CI-2 (PDB ID 2CI2), Eglin-c (elastase inhibitor of the leech *H. medicinalis*, PDB ID 1ACB), rBTI (PDB ID 3RDY), BGTI (bitter gourd trypsin inhibitor, PDB ID 1VBW), LUTI (*L. usitatissimum* trypsin inhibitor, PDB ID:1DWM), and CMTI-V (*C. maxima* trypsin inhibitor-V, PDB ID 1HYM) are aligned. The residues conserved with CI-2 are *shaded in blue*. The conserved residues among the other potato I family inhibitors are in *pale blue*. Cysteine residues are *highlighted in purple*. The residues in the binding loop are shown in the *red box*. The *black boxes* indicate residues that contribute to the stability of the binding loop.

itors are located in the binding loop. The residues at P_2, P_1', P_3', P_6', P_7', and P_8' are highly conserved in the potato I family inhibitors (Fig. 4).

Fig. 5 shows the superposition of the extended loop of AFUEI molecule A (Asp-41–Ile-48) onto the binding loop of CI-2 (Thr-55–Arg-62). The main chain atoms of the eight residues at the P_5-P_1 and P_1'-P_3' positions are superimposed with the root mean square deviation of 0.705 Å, suggesting that the loop conformation is almost identical between them. However the relative orientation of the loop against the molecular core is rather different (Fig. 5, *A* and *B*).

The conformation of the extended loop of AFUEI is stabilized by the hydrogen-bonding network between the core and the loop. The network pattern is slightly different between the two molecules (molecule A and B) in the asymmetric unit of the form II crystal (Fig. 6, *A* and *B*). In molecule A, the carbonyl oxygen atom of Glu-46 (P_1') in the loop interacts with the guanidino group of Arg-51 (P_6') in β3, and the conformation of the guanidino group is stabilized by the C-terminal carboxyl group of Ala-68. The carboxyl group also hydrogen-bonds with the main-chain nitrogen atom of Ile-48 (P_3') in the loop. The carbonyl oxygen atom of Thr-44 (P_2) and the main-chain nitrogen atom of Glu-46 (P_1') interact with Arg-35 in β2 through a water molecule (Fig. 6*A*). In molecule B, the side-chain carboxyl group of Glu-46 (P_1') interacts with the guanidino group of Arg-51 (P_6') directly, and Arg-35 interacts through a water molecule. The carbonyl oxygen atom of Thr-44 (P_2) also interacts with Arg-35 through the water molecule, but the position of the water molecule is slightly different from that in molecule A. The hydrogen-bonding network in AFUEI is similar to those of the potato I family inhibitors, such as CI-2 and rBTI (Fig. 6, *C* and *D*). In the CI-2 structure, the main-chain conformation of the P_1' and P_3' residues is stabilized by conserved interactions with the P_6' residue and the C-terminal carboxyl group. However, the P_2 residue is stabilized by slightly different manner.

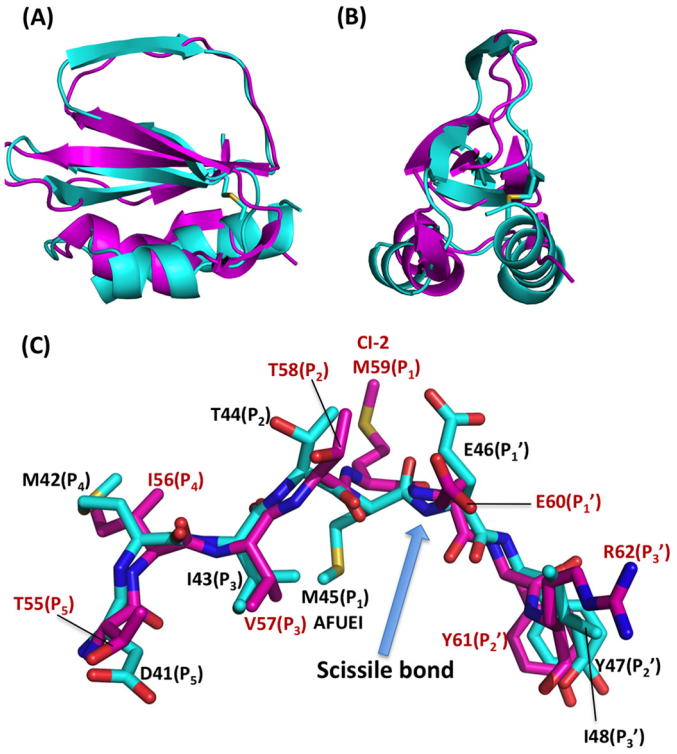

FIGURE 5. **Structural comparison of AFUEI and CI-2.** AFUEI (Form II molecule A) is superimposed to CI-2 by fitting the corresponding main chain atoms of the binding loop residues (from P_5 to P_3') with a root mean square deviation of 0.688. *A* and *B*, ribbon models of AFUEI and CI-2 (2CI2) are shown in *cyan* and *magenta*, respectively. *B*, shown is a side view (from the right) of *A*. *C*, shown is a close up view of the binding loop region represented by stick model. The carbon atoms of AFUEI are indicated by *cyan*, and those of CI-2 are in *magenta*. Oxygen, nitrogen, and sulfur atoms are colored in *red*, *blue*, and *yellow*, respectively.

The carbonyl oxygen atom of Thr-58 (P_2) directly interacts with Arg-67 (P_8') in β3.

The scissile bond is located between the P_1 and P_1' residues, and the P_1 residue is known to determine the specificity of the

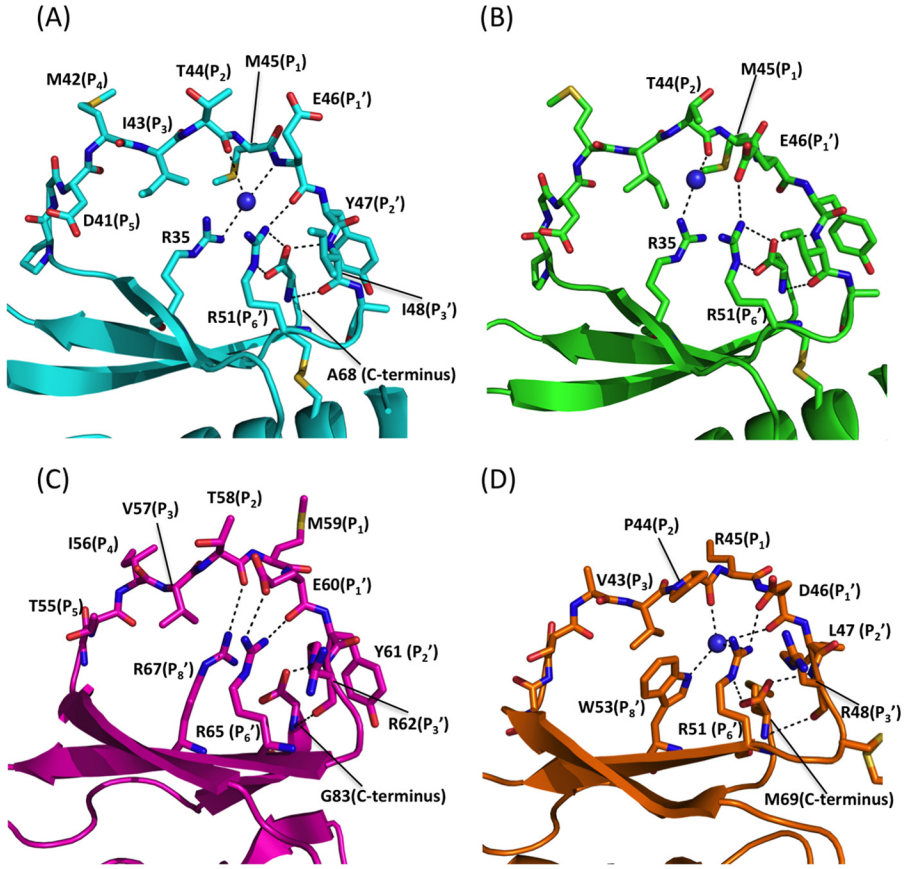

FIGURE 6. **Hydrogen-bonding network between the core and the binding loop.** Shown are AFUEI molecule A (*A*), AFUEI molecule B (*B*), CI-2 (*C*), and BTI (*D*). The residues in the binding loop and the residues involved in the network are shown in stick model. Hydrogen bonds are indicated by *black dotted lines*. The water molecules involved in the network are represented by *blue balls*.

inhibitor. The P_1 site residue of CI-2, which inhibits chymotrypsin-like and elastase-like proteases, is methionine. BTI inhibits trypsin-like proteases, and its P_1 site is arginine. The P_1 residue of AFUEI is methionine (Fig. 4 and 5), implying that AFUEI inhibits other chymotrypsin-like proteases but not trypsin-like proteases. We then examined its inhibitory activity toward some proteases (Table 3). AFUEI showed a high inhibitory activity against bovine α-chymotrypsin but had almost no activity against bovine trypsin. In agreement with previous results, AFUEI inhibited elastase from *A. flavus*, human leukocytes, and porcine pancreas. These results support the idea that AFUEI inhibits proteases in the same manner as the potato I family inhibitors.

Implication for the Inhibitory Mechanism of AFUEI—The inhibitory mechanism of the potato I family inhibitors, which is called the clogged gutter mechanism, has been proposed by Radisky and Koshland (24). In the proposed mechanism, the inhibitor quickly forms an acyl-enzyme intermediate with a protease, but the following steps go very slowly. The tight binding with the proper orientation of the leaving group peptide (H_2N-R′) to the protease prevents acyl-enzyme hydrolysis and product dissociation but promotes the reverse reaction. Thus, the hydrogen-bonding network that stabilizes the correct orientation of the binding loop is a key factor in this mechanism. In the CI-2 structure, Thr-58 (P_2), Glu-60 (P_1′), Arg-62 (P_3′), Arg-65 (P_6′), Arg-67 (P_8′), and the C-terminal carboxyl group (Gly-83) form a hydrogen bonding network. This network fixes the leaving group peptide to the molecular core with proper orientation. Mutational analysis of eglin-C indicated that P_2, P_1′, P_6′, and the C-terminal residues are essential for inhibition (36). Among the residues, the acidic P_1′ residue is crucial for resistance to proteolysis, and basic P_6′, P_3′, and P_8′ residues are important for tight binding to the protease (37). The hydrogen bonding network constructed by the C-terminal carboxyl group, P_6′ and P_1, tie the leaving group R′ peptide tightly to the protein core. These interactions prevent relegation of the leaving group and accelerate the reverse reaction.

TABLE 3
Inhibition activity of AFUEI

Protease	Absorbance (660 nm)	
	−AFUEI	+AFUEI
μg		
Chymotrypsin		
40	1.25	0.16
20	0.61	0.06
10	0.22	0.02
5	0.04	0.01
Trypsin		
10	0.75	0.71
4	0.42	0.33
2	0.19	0.19
1	0.07	0.07
Porcine elastase		
80	0.89	0.71
40	0.59	0.42
8	0.09	0.08
4	0.04	0.04

In AFUEI, the residues at P_2, P_1', and P_6' and the orientation of the C-terminal carboxyl group are conserved. The hydrogen-bonding network composed of the P_1' P_6', and P_3' residues and the C-terminal carboxyl group is similar to that of CI-2. The P_8' residue is not conserved, but Arg-35 with a water molecule plays a similar role to the arginine at P_8' in CI-2. Inclusion of a water molecule in the hydrogen-bonding network is also found in the rBTI structure (Fig. 6*D*) (22). Interestingly, rBTI changes its conformation upon binding to trypsin, and the water molecule is excluded from the network. It might be possible that AFUEI loses the water molecule when it binds to elastases. The arginine residue at the P_3' position is well conserved in the potato I family inhibitors but not in AFUEI. Although the arginine residue hydrogen-bonds with the P_5' residue located at the edge of β3, its contribution to the binding loop stability seems much less than the other two well conserved arginine residues (P_6' and P_8') (24).

Considering these observations together, we propose that AFUEI inhibits its cognate protease through the clogged gutter mechanism. The AFUEI structure strongly suggests a close relationship between the potato inhibitor I family (I13 inhibitor family) and the I78 inhibitor family.

Molecular Modeling of the Complex Structure of AFUEI and Human Neutrophil Elastase—The structural similarity with the potato inhibitor I family allowed us to construct a structure model of AFUEI in complex with HNE *in silico*. Two initial complex models, molecule A with HNE and molecule B with HNE, were built by using the rBTI-trypsin complex structure (PDB ID 3RDZ) as a template, and the models were then energy-minimized assuming the clogged gutter mechanism. The final model of the AFUEI (molecule A)-HNE complex is shown in Fig. 7. The overall structures of the final two models are almost same except for the side chain conformation of Met-45 (P_1) (supplemental Fig. S3), but the side chains of Met-45 in both molecules are properly accommodated in the hydrophobic active site pockets of HNE (supplemental Fig. S3*C*). Intermolecular main chain hydrogen bonds were suitably formed between AFUEI and HNE in both models (Fig. 7*B* and supplemental Fig. S3*C*). During the energy minimization, the water molecule between the extended loop and Arg-35/Arg-51 of AFUEI (Fig. 6, *A* and *B*) was excluded, and tight hydrogen bonds between Glu-46 (P_1') and Arg-51 (P_6') were formed, which may prevent hydrolysis of the binding loop like rBTI. These reasonable structural features of the complex model support that the inhibitory mechanism of AFUEI is similar to that of the potato I family inhibitors.

Phylogenic Analysis of Potato I Family Inhibitors and AFUEI—Multiple sequence alignment of the amino acid sequences of the potato I family inhibitors and AFUEI is shown in supplemental Fig. S1. A phylogeny of potato I family inhibitors and AFUEI was inferred from amino acid sequences of the inhibitors whose structures are known and their close homologues (Fig. 8 and supplemental Fig. S2). Because of high sequence diversities in several subfamilies of the inhibitors, it was difficult to accurately determine their phylogenetic relationships, *e.g.* branching order, at a large depth of the tree. However, the result obviously indicated rapid evolution of AFUEI from the other potato I family members, and this explained the reason why

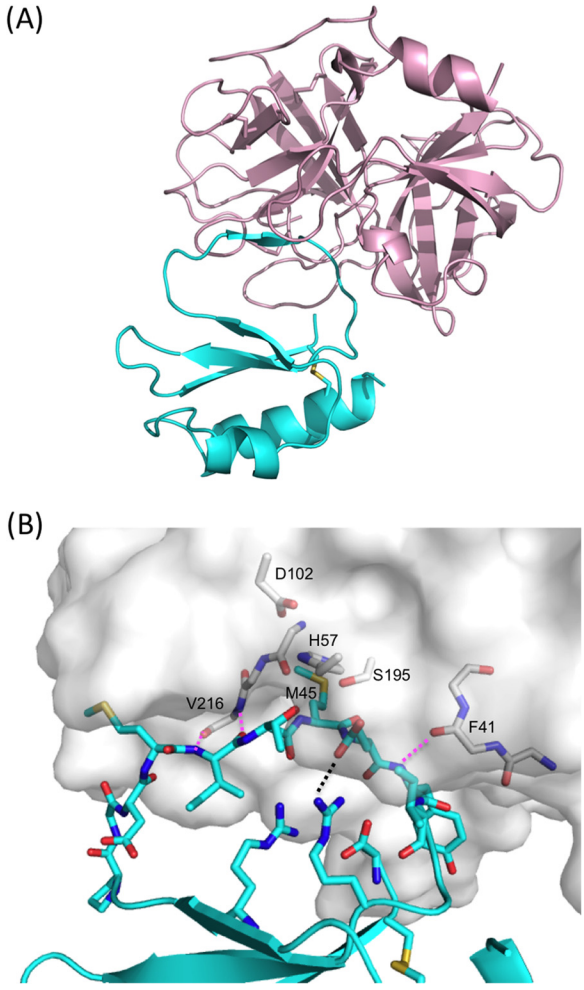

FIGURE 7. **Structure model of the AFUEI-HNE complex.** *A*, shown is a ribbon diagram of the AFUEI-HNE complex constructed by using molecule A in the form II crystal. AFUEI is shown in *cyan*, and HNE is in *pale pink*. *B*, shown is a close-up view of the interaction site of AFUEI with the molecular surface of HNE. The residues in the binding loop, the residues involved in the interaction between the core and the binding loop, and the S-S bond in AFUEI are indicated by the stick models whose carbon atoms are colored in *cyan*. The remaining part of AFUEI is represented by a ribbon model. The HNE residues of the catalytic triad (His-57, Asp-102, and Ser-195) and interacting with AFUEI are indicated by the stick models whose carbon atoms are colored in *white*. Hydrogen bonds between AFUEI and HNE are shown by a *pink dotted line*. The hydrogen bond between Glu-46 and Arg-51 are shown by a *black dotted line*.

homology between AFUEI and potato I family inhibitors from plants and annelid worms has not been detected. The tentative analysis of *dN*/*dS* implies high selection pressure among the families, which was also observed for several protease inhibitors (38, 39). The selection pressure was hypothesized to be necessary for establishing specificity between inhibitor and enzyme, and the result suggests that the highly deviated sequence of AFUEI may be attributed to a similar selection pressure.

The plant protease inhibitors play important roles in defense strategies in plants as shown in potato I family inhibitors (40). Some of them are included in the exudates of wounded plant cells and inhibit the proteases secreted by insects and many of the phytopathogenic microorganisms. Elastases produced by fungi of *Aspergillus* are thought to be major pathogenic factors in aspergillosis. AFUEI is thought to play an important role in defending proteolysis by its own elastase or by other proteases of the host organisms.

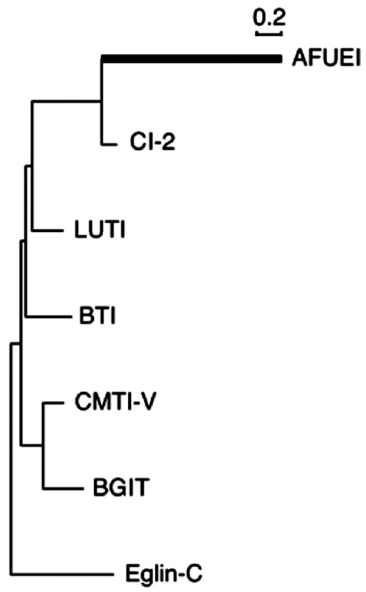

FIGURE 8. **Phylogenetic tree of the potato I family inhibitors.** Shown is the phylogenetic tree of the potato I family inhibitors whose three-dimensional structures are known. The tree lineage with a thick line depicts the *dN/dS* rate is greater than 1.0. The tree was drawn using the NJplot program. *LUTI*, *L. usitatissimum* trypsin inhibitor; *CMTI-V*, *C. maxima* trypsin inhibitor V; *BGIT*, bitter gourd trypsin inhibitor.

Acknowledgments—We thank Noriko Nishioka and Yoshiaki Yamada for technical assistance.

REFERENCES

1. Laskowski, M., Jr., and Kato, I. (1980) Protein inhibitors of proteinases. *Annu. Rev. Biochem.* **49,** 593–626
2. Rawlings, N. D., Barrett, A. J., and Bateman, A. (2012) MEROPS. The database of proteolytic enzymes, their substrates, and inhibitors. *Nucleic Acids Res.* **40,** D343–D350
3. Bouchara, J. P., Tronchin, G., Larcher, G., and Chabasse, D. (1995) The search for virulence determinants in *Aspergillus fumigatus*. *Trends Microbiol.* **3,** 327–330
4. Latgé, J. P. (1999) *Aspergillus fumigatus* and aspergillosis. *Clin Microbiol. Rev.* **12,** 310–350
5. Monod, M., Capoccia, S., Léchenne, B., Zaugg, C., Holdom, M., and Jousson, O. (2002) Secreted proteases from pathogenic fungi. *Int. J. Med. Microbiol.* **292,** 405–419
6. Alp, S., and Arikan, S. (2008) Investigation of extracellular elastase, acid proteinase, and phospholipase activities as putative virulence factors in clinical isolates of *Aspergillus* species. *J. Basic Microbiol.* **48,** 331–337
7. Gertler, A., and Hayashi, K. (1971) Esterolytic, elastase-like activity of purified alkaline proteinase from *Aspergillus sojae*. *Biochim. Biophys. Acta* **235,** 378–380
8. Feinstein, G., and Gertler, A. (1973) Isolation of alkaline proteinases from *Aspergillus oryzae* by one-step affinity chromatography on ovoinhibitor-Sepharose column. *Biochim. Biophys. Acta* **309,** 196–202
9. Morya, V. K., Yadav, S., Kim, E. K., and Yadav, D. (2012) *In silico* characterization of alkaline proteases from different species of *Aspergillus*. *Appl. Biochem. Biotechnol.* **166,** 243–257
10. Okumura, Y., Ogawa, K., Uchiya, K., and Nikai, T. (2006) Isolation and characterization of a novel elastase inhibitor, AFLEI, from *Aspergillus flavus*. *Nihon Ishinkin Gakkai Zasshi* **47,** 219–224
11. Okumura, Y., Ogawa, K., Uchiya, K., Komori, Y., Nonogaki, T., and Nikai, T. (2008) Biological properties of elastase inhibitor, AFLEI from *Aspergillus flavus*. *Nihon Ishinkin Gakkai Zasshi* **49,** 87–93
12. Okumura, Y., Matsui, T., Ogawa, K., Uchiya, K., and Nikai, T. (2008) Biochemical properties and primary structure of elastase inhibitor AFUEI from *Aspergillus fumigatus*. *J. Med. Microbiol.* **57,** 803–808
13. Okumura, Y., Ogawa, K., Uchiya, K., and Nikai, T. (2007) Characterization and primary structure of elastase inhibitor, AFLEI, from *Aspergillus flavus*. *Nihon Ishinkin Gakkai Zasshi* **48,** 13–18
14. Nikai, T., Sugihara, H., and Tanaka, T. (1977) Enzymochemical studies on snake venoms-II. Purification ot lethal protein Ac1-Proteinase in the venom of *Agkistrodon acutus*. *Yakugaku Zasshi.* **97,** 507–514
15. Rawlings, N. D. (2010) Peptidase inhibitors in the MEROPS database. *Biochimie* **92,** 1463–1483
16. Yamashita, N., Komori, Y., Okumura, Y., Uchiya, K., Matsui, T., Nishimura, A., Ogawa, K., and Nikai, T. (2011) High-yields heterologous production of the novel *Aspergillus fumigatus* elastase inhibitor AFUEI in *Aspergillus oryzae*. *J. Biosci. Bioeng.* **112,** 114–117
17. Leslie A. G. W. (1992) Recent changes to the MOSFLM package for processing film and image plate data. *CCP4 + ESF-EAMCB Newsletter Protein Crystallogr.* **26,** 27–33
18. Winn, M. D., Ballard, C. C., Cowtan, K. D., Dodson, E. J., Emsley, P., Evans, P. R., Keegan, R. M., Krissinel, E. B., Leslie, A. G., McCoy, A., McNicholas, S. J., Murshudov, G. N., Pannu, N. S., Potterton, E. A., Powell, H. R., Read, R. J., Vagin, A., and Wilson, K. S. (2011) Overview of the CCP4 suite and current developments. *Acta Crystallogr. D Biol. Crystallogr.* **67,** 235–242
19. Adams, P. D., Grosse-Kunstleve, R. W., Hung, L. W., Ioerger, T. R., McCoy, A. J., Moriarty, N. W., Read, R. J., Sacchettini, J. C., Sauter, N. K., and Terwilliger, T. C. (2002) PHENIX. Building new software for automated crystallographic structure determination. *Acta Crystallogr. D Biol. Crystallogr.* **58,** 1948–1954
20. Emsley, P., Cowtan, K. (2004) Coot. Model-building tools for molecular graphics. *Acta Crystallogr. D Biol. Crystallogr.* **60,** 2126–2132
21. Brünger, A. T., Adams, P. D., Clore, G. M., DeLano, W. L., Gros, P., Grosse-Kunstleve, R. W., Jiang, J. S., Kuszewski, J., Nilges, M., Pannu, N. S., Read, R. J., Rice, L. M., Simonson, T., and Warren, G. L. (1998) Crystallography and NMR system. A new software suite for macromolecular structure determination. *Acta Crystallogr. D Biol. Crystallogr.* **54,** 905–921
22. Wang, L., Zhao, F., Li, M., Zhang, H., Gao, Y., Cao, P., Pan, X., Wang, Z., and Chang, W. (2011) Conformational changes of rBTI from buckwheat upon binding to trypsin. Implications for the role of the P_8' residue in the potato inhibitor I family. *PLoS ONE* **6,** e20950
23. Koizumi, M., Fujino, A., Fukushima, K., Kamimura, T., Takimoto-Kamimura, M. (2008) Complex of human neutrophil elastase with 1/2SLPI. *J. Synchrotron Radiat.* **15,** 308–311
24. Radisky, E. S., and Koshland, D. E., Jr. (2002) A clogged gutter mechanism for protease inhibitors. *Proc. Natl. Acad. Sci. U.S.A.* **99,** 10316–10321
25. Altschul, S. F., Gish, W., Miller, W., Myers, E. W., and Lipman, D. J.,(1990) Basic local alignment search tool. *J. Mol. Biol.* **215,** 403–410
26. Frigerio, F., Coda, A., Pugliese, L., Lionetti, C., Menegatti, E., Amiconi, G., Schnebli, H. P., Ascenzi, P., and Bolognesi, M. (1992) Crystal and molecular structure of the bovine α-chymotrypsin-eglin c complex at 2.0 Å resolution. *J. Mol. Biol.* **225,** 107–123
27. McPhalen, C. A., James, M. N. (1987) Crystal and molecular structure of the serine proteinase inhibitor CI-2 from barley seeds. *Biochemistry* **26,** 261–269
28. Cierpicki, T., and Otlewski, J. (2000) Determination of a high precision structure of a novel protein, *Linum usitatissimum* trypsin inhibitor (LUTI), using computer-aided assignment of NOESY cross-peaks. *J. Mol. Biol.* **302,** 1179–1192
29. Cai, M., Gong, Y. X., Wen, L., and Krishnamoorthi, R. (2002) Correlation of binding-loop internal dynamics with stability and function in potato I inhibitor family. Relative contributions of Arg-50 and Arg-52 in *Cucurbita maxima* trypsin inhibitor-V as studied by site-directed mutagenesis and NMR spectroscopy. *Biochemistry* **41,** 9572–9579
30. Hijikata, A., Yura, K., Noguti, T., and Go, M. (2011) Revisiting gap locations in amino acid sequence alignments and a proposal for a method to improve them by introducing solvent accessibility. *Proteins* **79,** 1868–1877
31. Thompson, J. D., Higgins, D. G., and Gibson, T. J. (1994) ClustalW. Improving the sensitivity of progressive multiple sequence alignment through sequence weighting, position-specific gap penalties and weight matrix choice. *Nucleic Acids Res.* **22,** 4673–4680

32. Yang, Z. (2007) PAML 4. Phylogenetic analysis by maximum likelihood. *Mol. Biol. Evol.* **24,** 1586–1591
33. McPhalen, C. A., and James, M. N. (1988) Structural comparison of two serine proteinase-protein inhibitor complexes. Eglin-c-subtilisin Carlsberg and CI-2-subtilisin Novo. *Biochemistry* **27,** 6582–6598
34. Betzel, C., Dauter, Z., Genov, N., Lamzin, V., Navaza, J., Schnebli, H. P., Visanji, M., and Wilson, K. S. (1993) Structure of the proteinase inhibitor eglin c with hydrolyzed reactive centre at 2.0 Å resolution. *FEBS Lett.* **317,** 185–188
35. Wojtaszek, J., Kolaczkowska, A., Kowalska, J., Nowak, K., and Wilusz, T. (2006) LTCI, a novel chymotrypsin inhibitor of the potato I family from the earthworm *Lumbricus terrestris.* Purification, cDNA cloning, and expression. *Comp. Biochem. Physiol. B Biochem. Mol. Biol.* **143,** 465–472
36. Jackson, S. E., and Fersht, A. R. (1994) Contribution of residues in the reactive site loop of chymotrypsin inhibitor 2 to protein stability and activity. *Biochemistry* **33,** 13880–13887
37. Radisky, E. S., Lu, C. J., Kwan, G., and Koshland, D. E., Jr. (2005) Role of the intramolecular hydrogen bond network in the inhibitory power of chymotrypsin inhibitor 2. *Biochemistry* **44,** 6823–6830
38. Hill, R. E., and Hastie, N. D. (1987) Accelerated evolution in the reactive centre regions of serine protease inhibitors. *Nature* **326,** 96–99
39. Taguchi, S., Kojima, S., Terabe, M., Kumazawa, Y., Kohriyama, H., Suzuki, M., Miura, K., and Momose, H. (1997) Molecular phylogenetic characterization of *Streptomyces* protease inhibitor family. *J. Mol. Evol.* **44,** 542–551
40. Habib, H., and Fazilli, K. M. (2007) Plant protease inhibitors. A defense strategy in plants. *Biotechnology and Molecular Biology Review* **2,** 68–85